## Title

Brain atrophy in primary progressive aphasia involves the cholinergic basal forebrain and Ayala's nucleus



## Journal

Psychiatry Research, 221(3)

## ISSN

0165-1781

## Authors

Teipel, Stefan J
Flatz, Wilhelm
Ackl, Nibal
et al.

## Publication Date

2014-03-01

## DOI

10.1016/j.pscychresns.2013.10.003

Peer reviewed

Published in final edited form as:
*Psychiatry Res*. 2014 March 30; 221(3): 187–194. doi:10.1016/j.pscychresns.2013.10.003.

# Brain atrophy in primary progressive aphasia involves the cholinergic basal forebrain and Ayala's nucleus

**Stefan J. Teipel**[a,b,*], **Wilhelm Flatz**[c], **Nibal Ackl**[d], **Michel Grothe**[a,b], **Ingo Kilimann**[a,b], **Arun L.W. Bokde**[e], **Lea Grinberg**[f], **Edson Amaro Jr.**[g], **Vanja Kljajevic**[b], **Eduardo Alho**[h,i], **Christina Knels**[j], **Anne Ebert**[k], **Helmut Heinsen**[i], and **Adrian Danek**[d]

[a]Department of Psychosomatic Medicine, University Medicine Rostock, Gehlsheimer Str. 20, 18147 Rostock, Germany

[b]DZNE, German Center for Neurodegenerative Diseases, Rostock, Germany

[c]Department of Clinical Radiology, University Hospitals – Grosshadern, Ludwig-Maximilians Universität, Munich, Germany

[d]Department of Neurology, Ludwig-Maximilians Universität, Munich, Germany

[e]Discipline of Psychiatry, School of Medicine and Trinity College Institute of Neuroscience (TCIN), Laboratory of Neuroimaging & Biomarker Research, Trinity College Dublin, The Adelaide and Meath Hospital incorporating the National Children's Hospital (AMiNCH), Dublin, Ireland, UK

[f]Department of Pathology, University of Sao Paulo Medical School, Sao Paulo, Brazil

[g]Department of Radiology, University of Sao Paulo Medical School, Sao Paulo, Brazil

[h]Department of Neurosurgery, University of Sao Paulo Medical School, Sao Paulo, Brazil

[i]Morphological Brain Research Unit, Department of Psychiatry, University Würzburg, Würzburg, Germany

[j]Hochschule Fresenius, Hamburg, Germany

[k]Department of Neurology, University of Mannheim, Mannheim, Germany

## Abstract

Primary progressive aphasia (PPA) is characterized by left hemispheric frontotemporal cortical atrophy. Evidence from anatomical studies suggests that the nucleus subputaminalis (NSP), a subnucleus of the cholinergic basal forebrain, may be involved in the pathological process of PPA. Therefore, we studied the pattern of cortical and basal forebrain atrophy in 10 patients with a clinical diagnosis of PPA and 18 healthy age-matched controls using high-resolution magnetic resonance imaging (MRI). We determined the cholinergic basal forebrain nuclei according to Mesulam's nomenclature and the NSP in MRI reference space based on histological sections and



[*]Corresponding author at: Department of Psychosomatic Medicine, University Medicine Rostock, Gehlsheimer Str. 20, 18147 Rostock, Germany. Tel.: +49 381 494 9471; fax: +49 381 494 9472. stefan.teipel@med.uni-rostock.de (S.J. Teipel)..

**Appendix. Supplementary material**

Supplementary data associated with this article can be found in the online version at http://dx.doi.org/10.1016/j.pscychresns.2013.10.003.

the MRI scan of a post-mortem brain *in cranio*. Using voxel-based analysis, we found left hemispheric cortical atrophy in PPA patients compared with controls, including prefrontal, lateral temporal and medial temporal lobe areas. We detected cholinergic basal forebrain atrophy in left predominant localizations of Ch4p, Ch4am, Ch4al, Ch3 and NSP. For the first time, we have described the pattern of basal forebrain atrophy in PPA and confirmed the involvement of NSP that had been predicted based on theoretical considerations. Our findings may enhance understanding of the role of cholinergic degeneration for the regional specificity of the cortical destruction leading to the syndrome of PPA.

**Keywords**

Cholinergic system; Language; Primary progressive aphasia; Post-mortem MRI; Nucleus subputaminalis; Diagnosis

## 1. Introduction

Primary progressive aphasia (PPA) is a language-based dementia syndrome characterized by progressive loss of specific aspects of speech and language, whereas other cognitive domains are initially spared (Mesulam, 1982; Weintraub et al., 1990). Recently, the syndrome has been classified into three different variants, including a nonfluent/agrammatic variant, a semantic variant, and a logopenic variant (Gorno-Tempini et al., 2011). They differ in language production and comprehension deficit patterns, which appear to be associated with different cortical sites undergoing atrophic changes (Wilson et al., 2010).

The syndrome of PPA has been associated with a variety of neuropathologic diagnoses at autopsy, including frontotemporal lobar degeneration (FTLD) associated with abnormal deposits of the microtubule-associated protein τ (FTLD-τ) or of TDP43 (FTLD-TDP) (Mesulam et al., 2008; Bigio et al., 2010), and with Alzheimer's disease (AD) pathology. High-resolution magnetic resonance imaging (MRI) studies reveal cortical destruction in PPA in the cortical language areas such as the inferior frontal and lateral temporal lobe, with extension into the insular cortex and the frontal and parietal opercula (Rogalski et al., 2011a). Furthermore, atrophy of striatal and thalamic gray matter has been described in frontal temporal dementias, including cases with primary progressive aphasia (Chow et al., 2008).

Cortical cholinergic denervation has been widely described in AD, resulting from the atrophy and loss of corticopetal projecting cholinergic neurons of the basal forebrain (Mesulam, 2004). Based on neurobiological evidence, the cholinergic deficit may also play a role in primary progressive aphasia, even if this syndrome is part of the FTLD spectrum. More specifically, it has been hypothesized that language integrity crucially depends on the relative dopaminergic–cholinergic activity balance in the cerebral areas that are primary targets for dopaminergic (*e.g.*, supplementary motor area, which regulates speech initiation) and cholinergic (*e.g.*, temporal lobe) innervation (Tanaka and Bachman, 2000).

Furthermore, Broca's region, the anterior language area, is characterized by a rich cholinergic innervation (Amunts et al., 2010). Within the rostral-lateral extension of the

basal forebrain, a distinguished cluster of neurons has been termed nucleus subputaminalis (NSP) by Ayala (1915). So far, Ayala's nucleus has only been described in humans and anthropoid monkeys, but not in other species including nonanthropoid primates (Simic et al., 1999). The NSP exhibits a strong left laterality and is located in close proximity to the external capsule, suggesting a strong connectivity to the cortical speech areas. Together, these findings have raised the question whether the NSP may be related to language function in the human brain (Simic et al., 1999).

In the present study, we determined a pattern of cortical and subcortical atrophy in primary progressive aphasia compared to healthy control subjects using automated volumetric analysis of high-resolution MRI scans. We focused on the regional distribution of atrophy within the basal forebrain nuclei using a novel mask of the basal forebrain nuclei in MRI space based on a post-mortem MRI *in cranio* and subsequent histological study of a single subject. Elucidation of cholinergic system degeneration in primary progressive aphasia provides a potential target for future therapeutic interventions, and advances our understanding of the contribution of the cholinergic system, specifically the NSP, to language function in the human brain.

## 2. Methods

### 2.1. Subjects

We examined 10 right-handed patients with the clinical diagnosis of primary progressive aphasia (mean age 67.2 (S.D. 8.4) years, four women). Five subjects were diagnosed with the subtype of progressive nonfluent aphasia (PNFA), and five subjects with the subtype of semantic dementia (SD). Diagnoses were originally made according to the criteria of Neary et al. (1998). The PNFA patients correspond to the nonfluent/agrammatic variant, and the SD patients to the semantic variant of PPA as proposed by Gorno-Tempini et al. (2011). For comparison, we investigated 18 right-handed cognitively healthy elderly subjects (mean age 63.4 (S.D. 5.4) years, nine women).

PPA patients had undergone an extensive language and neuropsychological assessment (Knels and Danek, 2010), including the Aachener Aphasia Examination (Huber et al., 1983) and the Bogenhausen Semantic Test (BOSU) (Glindemann et al., 2002). We applied a measure of crystalline intelligence (Multiple Choice Intelligence Test, MWT-B) and the Consortium to Establish a Registry of Alzheimer's Disease (CERAD-Plus) battery, which included naming of line drawings from the Boston Naming Test as well as verbal learning and verbal fluency tasks. In addition, subjects were tested using verbal and nonverbal spans (Wechsler Memory Scale-Revised, WMS-R), nonverbal memory (Doors Test), clock drawing, and measures of executive function (Exit Interview, EXIT-25, formation of nonverbal concepts from LPS-3, Labyrinth test from the Neuropsychological Assessment Instrument (NAI), and Luria's alternate patterns) as well as calculation. The clinical examination also included tests for buccofacial and ideomotor apraxia and for the applause sign. The detailed neuropsychological test results of the PPA patients are summarized in Supplementary Table 1.

Healthy volunteers were spouses of our patients who had no subjective cognitive complaints, and scored within 1 S.D. of the age- and education-adjusted norm in all subtests of the CERAD cognitive battery (Berres et al., 2000) and the Trail Making Test Parts A and B (Chen et al., 2000). All controls received a score of 1 in the clock drawing test (Shulman et al., 1986). All healthy control subjects scored 0 in the Clinical Dementia Rating (CDR) (Morris, 1993).

The Mini-Mental-State Examination (MMSE) was used to assess the overall level of cognitive impairment (Folstein et al., 1975). The patient and control groups were not significantly different in age ($t$=1.47, d.f.=26, $p$=0.154) and gender distribution (Fisher's exact test, $p$=0.456). As expected, PPA patients had lower performance in the MMSE compared with controls (23.9 (S.D. 6.1) in PPA and 29.1 (S.D. 1.1) in controls, respectively; $t$= −3.37, d.f.=26, $p$=0.003).

The assessment of patients and healthy subjects included detailed medical history and examination, as well as laboratory tests (complete blood count, electrolytes, glucose, blood urea nitrogen, creatinine, liver-associated enzymes, cholesterol, high-density lipoproteins, triglycerides, serum B12, folate, thyroid function tests, coagulation, and serum iron).

The study was approved by the institutional review board of the Medical Faculty of the University of Munich. Written informed consent was obtained in every case before examination according to the Declaration of Helsinki.

### 2.2. Post-mortem brain

The delineation and localization of the cholinergic basal forebrain nuclei according to Mesulam's nomenclature, including the localization of the NSP in MRI reference space, were based on the histological serial coronal sections of a post-mortem brain from a 56-years-old man. The cause of death was myocardial infarct, and no previous neurological diseases were reported by the relatives. Before removal from the skull, the brain was scanned post-mortem *in cranio* (post-mortem interval 15 h 30 min) and for a second time after formalin fixation (1:9) for 3 months *ex cranio* at the Institute of Radiology of Sao Paulo Medical School on a 3.0T system (Philips Achieva) using an eight-channel head coil. Pathological findings were not detected in the post-mortem *in cranio* MR scan. All procedures were approved by the local Ethics Committee.

After formalin fixation, the brain was dehydrated in graded series of ethanol solutions. The dehydrated brain was scanned at the Institute of Radiology, University of Rostock on a 3T system (Siemens Magnetom Verio). After scanning, the rostral parts anterior to the anterior horn and dorsal parts of the frontal lobe were severed to facilitate histological processing. The remaining block was soaked in an 8% solution of celloidin and subjected to celloidin-mounting by means of a vacuum-assisted embedding procedure. Celloidin was hardened by chloroform vapors and finally by immersion in 70% alcohol. The celloidin block with the brain was serially cut on a sliding microtome (Polycut, Cambridge Instruments, UK) to a section thickness of 400 μm in the frontal plane. During sectioning, each newly appearing block surface was imaged with a digital single-lens reflex (DSLR) camera. Details of the procedure and its scope are given elsewhere (Grinberg et al., 2008, 2009). The serial 400-μm

celloidin sections were subsequently stained by a modified gallocyanin technique (Heinsen et al., 2000).

### 2.3. MRI acquisition

**2.3.1. In vivo scans—**MRI acquisitions of the brain were conducted with a 1.5 T scanner with parallel imaging capabilities (Magnetom Vision, Siemens, Erlangen, Germany), maximum gradient strength 25 mT/m, maximum slew rate 130 T/m/s, and quadrature detection head coil (transmit–receive circulary polarized CP-head coil).

For the anatomical study, a sagittal high-resolution three-dimensional gradient-echo sequence was performed (MPRAGE, field-of-view 250 mm, spatial resolution 1.0 × 1.0 × 1.0 $mm^3$, repetition time 11.4 ms, echo time 4.4 ms, inversion time 300 ms, flip angle 8°, and number of slices 160). To identify white matter lesions, a coronal two-dimensional T2-weighted sequence was performed (fluid attenuation inversion recovery, FLAIR, field-of-view 230 mm, repetition time 7000 ms, echo time 110 ms, inversion time 2500 ms, voxel size 0.9 × 0.9 × 5.0 $mm^3$, flip angle 180°, and number of slices 21).

**2.3.2. Post-mortem scans—**The *in cranio* MRI scans were acquired on a 3.0 T MR scanner (Achieva, Philips Medical Systems, Best, The Netherlands) using a sagittal 3D T1 fast field echo (FFE) sequence with 1-mm isotropic resolution (field-of-view 240 mm), a repetition time 7 ms, echo time 3.2 ms, flip angle 8°, and number of slices 180. An eight-channel head coil was used and the subject was positioned in supine position.

The MRI scans after alcohol dehydration were acquired on a 3.0 T MR scanner (Magnetom Verio, Siemens Medical Solutions, Erlangen, Germany) using a sagittal MPRAGE sequence with 1-mm isotropic resolution, repetition time 2500 ms, echo time 4.81 ms, inversion time 1100 ms, flip angle 7°, and number of slices 200. For scanning, the brain had been placed in an eight-channel knee coil.

### 2.4. MRI data processing

The processing of structural MRI scans was implemented through statistical parametric mapping, SPM8 (Wellcome Dept. of Imaging Neuroscience, London) and the VBM8-toolbox (http://dbm.neuro.uni-jena.de/vbm/) implemented in MATLAB 7.1 (Mathworks, Natwick, MA). First, images were segmented into gray matter (GM), white matter (WM) and cerebrospinal fluid (CSF) partitions using the tissue prior free segmentation routine of the VBM8-toolbox. The GM and WM partitions of each subject were then high-dimensionally registered to a crisp template of average anatomy in Montreal Neurological Institute (MNI) space (IXI template) using the Diffeomorphic Anatomic Registration using Exponentiated Lie algebra (DARTEL) algorithm (Ashburner, 2007). The IXI template is part of the VBM8-toolbox and was derived by DARTEL intersubject alignment of 550 healthy control subjects of the publicly available IXI Database (http://www.brain-development.org).

Flow-fields resulting from the DARTEL registration to the IXI template were used to warp the GM segments, and voxel values were modulated for nonlinear effects of the high-dimensional normalization. This preserves the total amount of GM volume after linear

effects of global head size and shape differences have been accounted for. Finally, modulated warped GM segments were resliced to an isotropic voxel-size of 1.5 $mm^3$ and smoothed with a Gaussian smoothing kernel of 8-mm full-width at half maximum (FWHM) for the analysis of cortical atrophy and a Gaussian smoothing kernel of 4 mm for the analysis of basal forebrain atrophy. Following the matched filter theorem, the optimal smoothing kernel in voxel-based analyses should be matched in size to the expected effects. The selection of the different smoothing kernels was based on the findings of our previous study where changes in the basal forebrain were better detected with univariate statistics using 4-mm smoothing than using 8-mm smoothing (Grothe et al., 2012).

### 2.5. Post-mortem map

Fig. 1 illustrates the processing of the post-mortem MRI data. Subregions of the cholinergic nuclei were identified from digitalized stained sections of the basal forebrain and manually transferred into the corresponding slices of the post-mortem MRI of the dehydrated brain in alcohol space. SPM8 (Wellcome Trust Centre for Neuroimaging, London, UK. Available from: http://www.fil.ion.ucl.ac.uk/spm) was applied to the MRI brain volume in alcohol space, which was transferred into the post-mortem *in cranio* MRI space with a 12-parameter affine transformation followed by high-dimensional normalization (Ashburner et al., 1999). In a further step, the post-mortem *in cranio* MRI was transferred into stereotaxic coordinates in MNI standard space with the Diffeomorphic Anatomic Registration using Exponentiated Lie algebra (DARTEL) registration method (Ashburner, 2007). The linear and nonlinear transformations from alcohol through *in cranio* to MNI space were combined to spatially transform the basal forebrain mask into the MNI standard space. We used this map to relate the group effects in local deformations to the anatomical position of the basal forebrain nuclei in MNI space.

### 2.6. Statistical analysis

We used two complementary analytics approaches, (i) voxel-based and (ii) region of interest analysis.

- **i.** For the voxel-based analysis, we employed the general linear model within the SPM framework. We determined between-group differences in GM volume between the PPA patients and the control subjects for the GM maps smoothed with an 8-mm kernel, and for the GM maps smoothed with a 4-mm kernel and masked for the basal forebrain regions. For the cortical atrophy analysis, results were thresholded at $p < 0.001$ with a minimum cluster extension threshold of 50 contiguous voxels (corresponding to a volume of 168.75 $mm^3$). Given the *a priori* hypothesis and the very small search region of probably highly interdependent voxel-values, the basal forebrain results were assessed at an uncorrected statistical threshold of $p < 0.01$ with a minimum cluster extent threshold of 5 contiguous voxels (16.88 $mm^3$).
- **ii.** For the region of interest analysis, we summed the GM volume within each of the cholinergic basal forebrain nuclei and compared the average GM volumes between groups using a multivariate linear model followed with two-sample independent *t*-

tests, thresholded at $p < 0.05$ with the Bonferroni correction for 12 independent comparisons (six regions in two hemispheres).

## 3. Results

### 3.1. Cortical GM atrophy in PPA compared with controls

Using univariate regression, we found left hemispheric reductions of cortical GM volume in PPA patients compared with controls in large clusters extending from the superior and inferior frontal gyri across the anterior temporal poles, lateral temporal cortex, insula, and parahippocampal gyrus to the cuneus (Table 1 and Fig. 2a).

In addition to the analysis of the entire PPA group, we determined the pattern of cortical GM atrophy separately for the PNFA and SD subgroups. When we masked the atrophy of the SD subgroup for the atrophy effects within the PNFA subgroup, we found left hemispheric areas in the temporal pole, lateral temporal cortex, Heschl's gyrus, the insula cortex, and the parahippocampal gyrus that were exclusively related to the atrophy in the SD group. When we masked the atrophy of the PNFA subgroup for the atrophy effects within the SD subgroup, we found areas in the superior and middle frontal gyrus as well as the supplementary motor cortex and cingulate gyrus that were exclusively related to the atrophy in the PNFA group (Fig. 2b).

### 3.2. Basal forebrain atrophy in voxel-based analysis

Univariate analysis of GM volume maps smoothed at 4 mm revealed a left predominant pattern of basal forebrain atrophy, including regions projecting on Ch3, Ch4am-al, Ch4p and NSP in the left hemisphere, and small effects in regions projecting on Ch4am-al, Ch4p and NSP in the right hemisphere (Fig. 3b). The pattern of atrophy was very similar when we compared GM volume separately between the PNFA subgroup and controls and between the SD subgroup and controls, respectively. Using masking of the between-group effects by either subgroup revealed no exclusive areas of atrophy for the SD or the PNFA subgroups within the basal forebrain region.

### 3.3. Region of interest analysis of the basal forebrain

Volumes of cholinergic nuclei were significantly different for all six subregions in both hemispheres with the exception of the right juxtacommissural region ($p < 0.016$), at a Bonferroni-corrected level of significance of $p$ ($\alpha$=0.05)=0.0042 (Fig. 4). In the Receiver Operating Characteristic (ROC) analysis, left Ch3 yielded an area under the curve (AUC) of 1, indicating perfect separation, followed by left Ch4p and left NSP with AUC of 0.983. AUCs for the right hemispheric nuclei were numerically smaller than the corresponding values of the left hemisphere throughout, but confidence intervals widely overlapped, thus indicating no significant differences in the extent of regional atrophy.

When we compared PNFA vs. control subjects using the nonparametric Mann–Whitney *U* tests, we found significant atrophy ($p < 0.05$) in all subregions except the right juxtacommissural region; in addition, effects in left Ch2 ($p < 0.009$), left Ch4am_l ($p <$

0.009), right Ch3 ($p < 0.009$) and right Ch4am_l ($p < 0.019$) did not survive the (conservative) Bonferroni correction for 12 comparisons.

For SD subjects, effects were significant for all subregions, except the left juxtacommissural area ($p$ 0.08); in addition, effects in the right juxtacommissural region=($p < 0.009$) and the right NSP ($p < 0.007$) did not survive the (conservative) Bonferroni correction for 12 comparisons.

BFCS volumes did not differ significantly between the SD and PNFA groups ($p > 0.15$ for all comparisons).

## 4. Discussion

We studied the pattern of cortical and subcortical atrophy in patients with PPA compared with healthy age-matched controls. Our primary aim was to determine the involvement of the nucleus subputaminalis (NSP) (Ayala, 1915) in PPA following hypotheses on the involvement of the NSP in language function in the human brain (Simic et al., 1999; Boban et al., 2006). Our secondary endpoint was to determine the involvement of basal forebrain cholinergic nuclei outside the NSP (Mesulam and Geula, 1988) in PPA. In addition, we used voxel-based analysis of cortical GM atrophy to characterize our sample with predominant left hemispheric involvement in agreement with the clinical diagnosis of PPA.

### 4.1. Pattern of cortical atrophy

We found left hemispheric cortical atrophy in lateral temporal, medial temporal, and prefrontal cortical areas as well as in cingulate GM areas in PPA patients compared with controls. The pattern of cortical atrophy in our PPA patients agrees with findings from previous studies (Fukui and Kertesz, 2000; Mesulam et al., 2012; Pereira et al., 2009; Rogalski et al., 2011b; Rohrer et al., 2009; Rosen et al., 2002). The seminal study by Gorno-Tempini et al. (2004) has shown differences in cortical atrophy between subtypes of primary progressive aphasia, including semantic dementia (SD) and progressive nonfluent aphasia (PNFA). Consistent with this previous evidence (Gorno-Tempini et al., 2004), our PNFA subjects showed exclusive involvement of the middle and superior frontal gyrus, and the cingulate gyrus, similar to a study on cortical thinning in subtypes of primary progressive aphasia (Rohrer et al., 2009). Our SD subjects showed exclusive effects in the anterior temporal pole and the lateral temporal cortex, similar to the previous study (Gorno-Tempini et al., 2004).

### 4.2. Atrophy of NSP

In agreement with our primary hypothesis, we found left hemispheric predominant atrophy of NSP in PPA as compared with healthy controls. Based on work by Simic et al. (1999), we hypothesized that Ayala's nucleus (NSP) might be involved in the atrophic process of PPA, since this nucleus appears to have a distinct association with language function; it has only been described in humans and anthropoid monkeys, but not in nonanthropoid primates or other mammals. It has a left hemispheric predominance and is located in close proximity to the cortical speech areas. In reference to a post-mortem mask of basal forebrain cholinergic

nuclei, we found widespread reductions in basal forebrain regions projecting on the localization of Ch3, Ch4am-al, Ch4p and NSP with a strong left hemispheric predominance.

This is the first study on basal forebrain atrophy in PPA. Simic et al. (1999, p. 85) had concluded their fundamental work on Ayala's nucleus with the following hypothesis: "It would be particularly interesting to investigate the role of the NSP in the primary progressive aphasia (PPA). […] We hypothesize that the pathological changes of the subputaminal nucleus may represent a missing substrate of " primary progressive aphasia, slowly progressive anarthria and AD. Our findings support the notion that the NSP is involved in progressive aphasia syndromes. The effects were, however, widespread within the basal forebrain and involved other basal forebrain subnuclei.

### 4.3. Atrophy of cholinergic basal forebrain beyond NSP

We found atrophy in basal forebrain areas beyond the NSP, corresponding to the locations of nucleus basalis Meynert subnuclei Ch3, Ch4am-al, and Ch4. Cholinergic system changes in FTLD have been the focus of only a few studies so far. Moon et al. (2008) measured the thickness of the substantia innominata (SI) on a single coronal section at the level of the anterior commissure as a proxy for atrophy of the nucleus basalis Meynert in patients with FTLD and AD. When compared with findings in age-matched controls, thickness of the (right) SI was significantly reduced in patients with AD but not in the FTLD group. However, this two-dimensional measurement of the SI at the level of the anterior commissure only provides a very gross estimate for atrophy of the forebrain cholinergic nuclei, which extend about 20 mm in the anterior–posterior direction. Moreover, the FTLD group only included three patients with PPA (one with SD and two with PNFA). Another approach to understanding the role of cholinergic dysfunction in PPA is provided by treatment studies using acetylcholinesterase inhibitors. Over a short period of 8 weeks, galantamine compared with placebo showed a trend towards stabilization of language function and global cognition in a small sample of PPA patients ($n$ = 10 verum and $n$ = 10 placebo) (Kertesz et al., 2008). An open label study showed improved behavioral symptoms in 20 subjects with the diagnosis of FTLD treated with rivastigmine compared with 20 untreated FTLD subjects over 12 months. Part of these effects may be due to underlying AD pathology in a subset of the patients (Mendez, 2009; Vossel and Miller, 2008). Injecting 0.4–0.6 mg of scopolamine disrupted cholinergic activity in healthy young women, leading to impairments in reading, writing, verbal fluency and object naming (Aarsland et al., 1994). This further supports the hypothesis that cholinergic depletion affects language. While cholinergic markers have been studied post-mortem in the behavior variant of FTLD without evidence of major alterations (Procter et al., 1999), we are not aware of a post-mortem study on cholinergic markers in PPA.

We do not have post-mortem data on the underlying nature of pathological changes in our PPA patients. Previous evidence suggests that it is the localization of a pathological lesion rather than its exact nature that determines the clinical phenotype (Weintraub and Mesulam, 2009). Accordingly, Pereira et al. (2009) have shown that the pattern of cortical atrophy is associated with the clinical phenotype but not the pathological phenotype in frontotemporal lobar degeneration including PNFA and SD. TDP43, ubiquitin and τ pathology of the FTLD

type, but also AD pathology, have been found associated with different subtypes of PPA with some degree of predilection (logopenic variant more likely to have AD pathology, semantic dementia more likely to have ubiquitin inclusions) but no strict separation (Davies et al., 2005; Kertesz and Munoz, 2002; Mesulam et al., 2008). Therefore, our data suggest that the clinical phenotype of PPA is associated with an involvement of basal forebrain cholinergic nuclei including NSP irrespective of the underlying pathological substrate.

### 4.4. Limitations

Our study has several limitations. First, the number of PPA subjects is small. Our results, however, encourage the study of a larger sample to determine the structural connectivity of the NSP and to replicate our findings. Furthermore, it will be interesting to correlate specific dimensions of speech and language impairment with the pattern of cholinergic atrophy in a larger number of PPA subjects. Second, the post-mortem mask of our study is based on only a single brain. We compared the distribution of our mask with the distribution of two previous masks, one based on a single subject (Teipel et al., 2005) and one probabilistic map based on 10 subjects (Zaborszky et al., 2008). There was a high general agreement between all three masks, with the only major difference being that Ch4p was located more ventrally in the first mask (Teipel et al., 2005) compared with the probabilistic mask (thresholded at 50%) (Zaborszky et al., 2008) and our new mask. These findings suggest that the anatomy of the basal forebrain nuclei is relatively stable across subjects. A particularly interesting feature of our new mask is that it is the only basal forebrain mask that has been developed in reference to the *in cranio* space. The signal distribution in high-resolution post-mortem MRI scans *in cranio* resembles the signal distribution *in vivo* (Ewers et al., 2011; Grinberg et al., 2008), thus allowing an accurate high-dimensional transformation from post-mortem into MNI standard space. Still, as we cannot directly see the basal forebrain nuclei in our analysis, some degree of uncertainty remains when outlining single nuclei. Finally, our sample consists of two clinically defined subtypes of PPA that may be related to different pathological substrates. We did not find clear differences in the pattern of cholinergic basal forebrain atrophy between PNFA and SD subjects. The limited number of subjects, however, precludes drawing firm conclusions from this lack of an effect.

### 4.5. Summary

In summary, for the first time we described the pattern of basal forebrain atrophy in PPA using a post-mortem mask of cholinergic subnuclei. We have determined the location of the NSP in MNI space and confirmed its involvement in PPA, as had already been suggested by Simic et al. (1999) based on theoretical considerations. Our findings strongly support the notion that the cholinergic basal forebrain warrants further study in larger samples as its region-specific involvement may enhance understanding of the regional specificity of the cortical destruction leading to the syndrome of PPA. Future studies may determine whether measurement of basal forebrain atrophy may help to differentiate among the types of pathology underlying the specific subtypes of the PPA syndrome.

## Supplementary Material

Refer to Web version on PubMed Central for supplementary material.

## References


Aarsland D, Larsen JP, Reinvang I, Aasland AM. Effects of cholinergic blockade on language in healthy young women. Implications for the cholinergic hypothesis in dementia of the Alzheimer type. Brain. 1994; 117(Pt. 6):1377–1384. [PubMed: 7820573]

Amunts K, Lenzen M, Friederici AD, Schleicher A, Morosan P, Palomero-Gallagher N, Zilles K. Broca's region: novel organizational principles and multiple receptor mapping. PLoS Biology. 2010; 8:pii: e1000489. http://dx.doi.org/10.1371/journal.pbio.1000489.

Ashburner J. A fast diffeomorphic image registration algorithm. NeuroImage. 2007; 38:95–113. [PubMed: 17761438]

Ashburner J, Andersson JL, Friston KJ. High-dimensional image registration using symmetric priors. NeuroImage. 1999; 9:619–628. [PubMed: 10334905]

Ayala G. A hitherto undifferentiated nuclues in the basla forebrain (nucleus subputaminalis). Brain. 1915; 37:433–438.

Berres M, Monsch AU, Bernasconi F, Thalmann B, Stahelin HB. Normal ranges of neuropsychological tests for the diagnosis of Alzheimer's disease. Studies in Health Technology and Informatics. 2000; 77:195–199. [PubMed: 11187541]

Bigio EH, Mishra M, Hatanpaa KJ, White CL 3rd, Johnson N, Rademaker A, Weitner BB, Deng HX, Dubner SD, Weintraub S, Mesulam M. TDP-43 pathology in primary progressive aphasia and frontotemporal dementia with pathologic Alzheimer disease. Acta Neuropathologica. 2010; 120:43–54. [PubMed: 20361198]

Boban M, Kostovic I, Simic G. Nucleus subputaminalis: neglected part of the basal nucleus of Meynert. Brain. 2006; 129:E42. (Author reply E43). [PubMed: 16543395]

Chen P, Ratcliff G, Belle SH, Cauley JA, DeKosky ST, Ganguli M. Cognitive tests that best discriminate between presymptomatic AD and those who remain nondemented. Neurology. 2000; 55:1847–1853. [PubMed: 11134384]

Chow TW, Izenberg A, Binns MA, Freedman M, Stuss DT, Scott CJ, Ramirez J, Black SE. Magnetic resonance imaging in frontotemporal dementia shows subcortical atrophy. Dementia and Geriatric Cognitive Disorders. 2008; 26:79–88. [PubMed: 18617738]

Davies RR, Hodges JR, Kril JJ, Patterson K, Halliday GM, Xuereb JH. The pathological basis of semantic dementia. Brain. 2005; 128:1984–1995. [PubMed: 16000337]

Ewers M, Frisoni GB, Teipel SJ, Grinberg LT, Amaro E Jr. Heinsen H, Thompson PM, Hampel H. Staging Alzheimer's disease progression with multimodality neuroimaging. Progress in Neurobiology. 2011; 95:535–546. [PubMed: 21718750]

Folstein MF, Folstein SE, McHugh PR. Mini-mental-state: a practical method for grading the cognitive state of patients for the clinician. Journal of Psychiatric Research. 1975; 12:189–198. [PubMed: 1202204]

Fukui T, Kertesz A. Volumetric study of lobar atrophy in Pick complex and Alzheimer's disease. Journal of Neurological Science. 2000; 174:111–121.

Glindemann, R.; Klintwort, D.; Ziegler, W.; Goldenberg, G. Bogenhausener Semantik-Untersuchung BOSU. Urban & Fischer; Munich, Germany: 2002.

Gorno-Tempini ML, Dronkers NF, Rankin KP, Ogar JM, Phengrasamy L, Rosen HJ, Johnson JK, Weiner MW, Miller BL. Cognition and anatomy in three variants of primary progressive aphasia. Annals of Neurology. 2004; 55:335–346. [PubMed: 14991811]

Gorno-Tempini ML, Hillis AE, Weintraub S, Kertesz A, Mendez M, Cappa SF, Ogar JM, Rohrer JD, Black S, Boeve BF, Manes F, Dronkers NF, Vandenberghe R, Rascovsky K, Patterson K, Miller BL, Knopman DS, Hodges JR, Mesulam MM, Grossman M. Classification of primary progressive aphasia and its variants. Neurology. 2011; 76:1006–1014. [PubMed: 21325651]

Grinberg LT, Amaro E Jr. Teipel S, dos Santos DD, Pasqualucci CA, Leite RE, Camargo CR, Goncalves JA, Sanches AG, Santana M, Ferretti RE, Jacob-Filho W, Nitrini R, Heinsen H. Assessment of factors that confound MRI and neuropathological correlation of human postmortem brain tissue. Cell Tissue Bank. 2008; 9:195–203. [PubMed: 18548334]

Grinberg LT, Amaro E Junior, da Silva AV, da Silva RE, Sato JR, dos Santos DD, de Paula Pacheco S, de Lucena Ferretti RE, Paraizo Leite RE, Pasqualucci CA, Teipel SJ, Flatz WH, Heinsen H.

Improved detection of incipient vascular changes by a biotechnological platform combining post mortem MRI in situ with neuropathology. Journal of Neurological Science. 2009; 283:2–8.

Grothe M, Heinsen H, Teipel SJ. Atrophy of the cholinergic basal forebrain over the adult age range and in early stages of Alzheimer's disease. Biological Psychiatry. 2012; 71:805–813. [PubMed: 21816388]

Heinsen H, Arzberger T, Schmitz C. Celloidin mounting (embedding without infiltration) – a new, simple and reliable method for producing serial sections of high thickness through complete human brains and its application to stereological and immunohistochemical investigations. Journal of Chemical Neuroanatomy. 2000; 20:49–59. [PubMed: 11074343]

Huber, W.; Poeck, K.; Weniger, D.; Willmes, K. Aachener Aphasie Test. Hogrefe; Göttingen, Germany: 1983.

Kertesz A, Morlog D, Light M, Blair M, Davidson W, Jesso S, Brashear R. Galantamine in frontotemporal dementia and primary progressive aphasia. Dementia and Geriatric Cognitive Disorders. 2008; 25:178–185. [PubMed: 18196898]

Kertesz A, Munoz DG. Primary progressive aphasia: a review of the neurobiology of a common presentation of Pick complex. American Journal of Alzheimer's Disease and Other Dementias. 2002; 17:30–36.

Knels C, Danek A. Loss of word-meaning with spared object semantics in a case of mixed primary progressive aphasia. Brain and Language. 2010; 113:96–100. [PubMed: 20034661]

Mendez MF. Frontotemporal dementia: therapeutic interventions. Frontiers in Neurology and Neuroscience. 2009; 24:168–178.

Mesulam M. The cholinergic lesion of Alzheimer's disease: pivotal factor or side show? Learning and Memory. 2004; 11:43–49. [PubMed: 14747516]

Mesulam M, Wicklund A, Johnson N, Rogalski E, Leger GC, Rademaker A, Weintraub S, Bigio EH. Alzheimer and frontotemporal pathology in subsets of primary progressive aphasia. Annals of Neurology. 2008; 63:709–719. [PubMed: 18412267]

Mesulam MM. Slowly progressive aphasia without generalized dementia. Annals of Neurology. 1982; 11:592–598. [PubMed: 7114808]

Mesulam MM, Geula C. Nucleus basalis (Ch4) and cortical cholinergic innervation in the human brain: observations based on the distribution of acetylcholinesterase and choline acetyltransferase. Journal of Comparative Neurology. 1988; 275:216–240. [PubMed: 3220975]

Mesulam MM, Wieneke C, Thompson C, Rogalski E, Weintraub S. Quantitative classification of primary progressive aphasia at early and mild impairment stages. Brain. 2012; 135:1537–1553. [PubMed: 22525158]

Moon WJ, Kim HJ, Roh HG, Han SH. Atrophy measurement of the anterior commissure and substantia innominata with 3 T high-resolution MR imaging: does the measurement differ for patients with frontotemporal lobar degeneration and Alzheimer disease and for healthy subjects? AJNR: American Journal of Neuroradiology. 2008; 29:1308–1313. [PubMed: 18436612]

Morris JC. The Clinical Dementia Rating (CDR): current version and scoring rules. Neurology. 1993; 43:2412–2414. [PubMed: 8232972]

Neary D, Snowden JS, Gustafson L, Passant U, Stuss D, Black S, Freedman M, Kertesz A, Robert PH, Albert M, Boone K, Miller BL, Cummings J, Benson DF. Frontotemporal lobar degeneration: a consensus on clinical diagnostic criteria. Neurology. 1998; 51:1546–1554. [PubMed: 9855500]

Pereira JM, Williams GB, Acosta-Cabronero J, Pengas G, Spillantini MG, Xuereb JH, Hodges JR, Nestor PJ. Atrophy patterns in histologic vs clinical groupings of frontotemporal lobar degeneration. Neurology. 2009; 72:1653–1660. [PubMed: 19433738]

Procter AW, Qurne M, Francis PT. Neurochemical features of frontotemporal dementia. Dementia and Geriatric Cognitive Disorders. 1999; 10(Suppl. 1):80–84. [PubMed: 10436347]

Rogalski E, Cobia D, Harrison TM, Wieneke C, Thompson CK, Weintraub S, Mesulam MM. Anatomy of language impairments in primary progressive aphasia. Journal of Neuroscience. 2011a; 31:3344–3350. [PubMed: 21368046]

Rogalski E, Cobia D, Harrison TM, Wieneke C, Weintraub S, Mesulam MM. Progression of language decline and cortical atrophy in subtypes of primary progressive aphasia. Neurology. 2011b; 76:1804–1810. [PubMed: 21606451]

Rohrer JD, Warren JD, Modat M, Ridgway GR, Douiri A, Rossor MN, Ourselin S, Fox NC. Patterns of cortical thinning in the language variants of frontotemporal lobar degeneration. Neurology. 2009; 72:1562–1569. [PubMed: 19414722]

Rosen HJ, Kramer JH, Gorno-Tempini ML, Schuff N, Weiner M, Miller BL. Patterns of cerebral atrophy in primary progressive aphasia. American Journal of Geriatric Psychiatry. 2002; 10:89–97. [PubMed: 11790639]

Shulman KI, Shedletsky R, Silver IL. The challenge of time: clock drawing and cognitive function in the elderly. International Journal of Geriatric Psychiatry. 1986; 1:135–140.

Simic G, Mrzljak L, Fucic A, Winblad B, Lovric H, Kostovic I. Nucleus subputaminalis (Ayala): the still disregarded magnocellular component of the basal forebrain may be human specific and connected with the cortical speech area. Neuroscience. 1999; 89:73–89. [PubMed: 10051218]

Talairach, J.; Tournoux, P. Co-Planar Stereotaxic Atlas of the Human BrainThieme. New York: 1988.

Tanaka, Y.; Bachman, DL. Pharmacotherapy of aphasia. In: Albert, ML.; Connor, LT.; Obler, LK., editors. Neurobehavior of Language and Cognition. Kluwer Academic Publishers; Norwell, MA: 2000. p. 159-176.

Teipel SJ, Flatz WH, Heinsen H, Bokde AL, Schoenberg SO, Stockel S, Dietrich O, Reiser MF, Moller HJ, Hampel H. Measurement of basal forebrain atrophy in Alzheimer's disease using MRI. Brain. 2005; 128:2626–2644. [PubMed: 16014654]

Vossel KA, Miller BL. New approaches to the treatment of frontotemporal lobar degeneration. Current Opinions in Neurology. 2008; 21:708–716.

Weintraub S, Mesulam M. With or without FUS, it is the anatomy that dictates the dementia phenotype. Brain. 2009; 132:2906–2908. [PubMed: 19861505]

Weintraub S, Rubin NP, Mesulam MM. Primary progressive aphasia. Longitudinal course, neuropsychological profile, and language features. Archives of Neurology. 1990; 47:1329–1335. [PubMed: 2252450]

Wilson SM, Henry ML, Besbris M, Ogar JM, Dronkers NF, Jarrold W, Miller BL, Gorno-Tempini ML. Connected speech production in three variants of primary progressive aphasia. Brain. 2010; 133:2069–2088. [PubMed: 20542982]

Zaborszky L, Hoemke L, Mohlberg H, Schleicher A, Amunts K, Zilles K. Stereotaxic probabilistic maps of the magnocellular cell groups in human basal forebrain. NeuroImage. 2008; 42:1127–1141. [PubMed: 18585468]

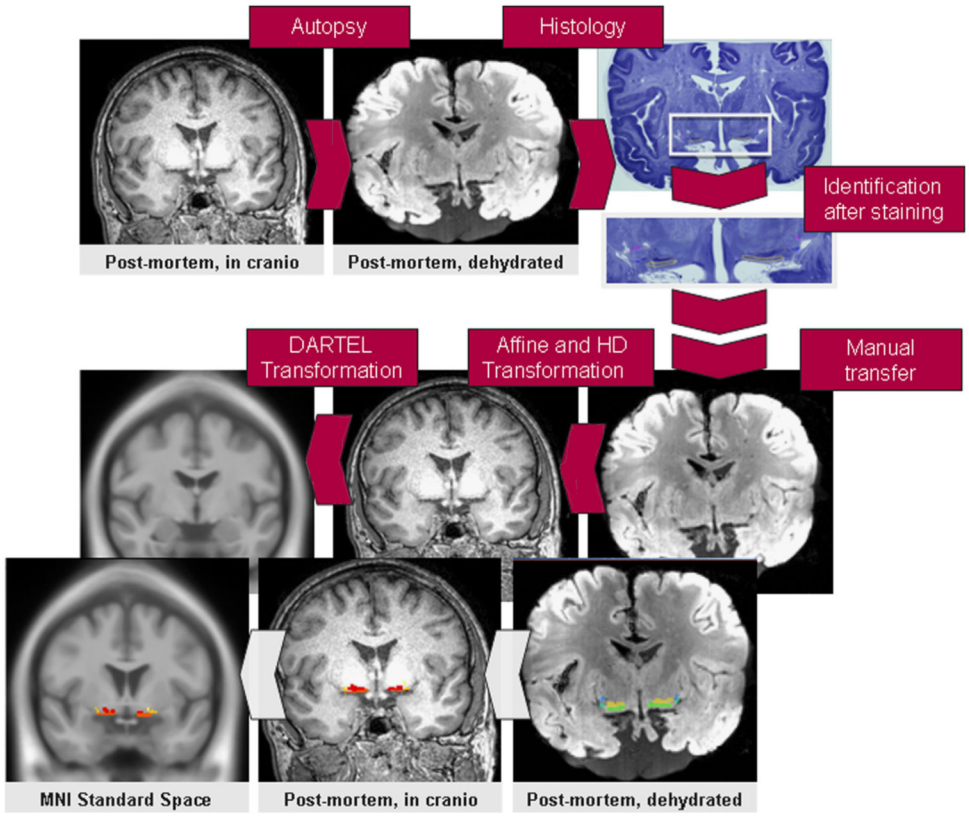


**Fig. 1.**

Transferring the localizations of cholinergic basal forebrain nuclei into the Montreal Neurological Institute (MNI) standard space. The brain of a 56-years-old man was scanned using MRI post-mortem *in cranio* and after alcohol dehydratation; thereafter, it was histologically stained to define the localization of basal forebrain cholinergic nuclei (first row). The histologically stained localizations of the cholinergic nuclei were manually transferred to the corresponding MRI sections from the dehydrated brain (last row, right image). Using 12-parameter affine and high dimensional (HD) nonlinear normalization, the MRI in alcohol space was spatially realigned to the brain in *in cranio* space (middle row, middle image). The *in cranio* MRI again was spatially normalized to MNI space using DARTEL (middle row, left image). The combined transformation parameters from alcohol to *in cranio* space and from *in cranio* to MNI space were applied to the cholinergic basal forebrain mask to obtain a mask in MNI standard space (last row, middle and right image).

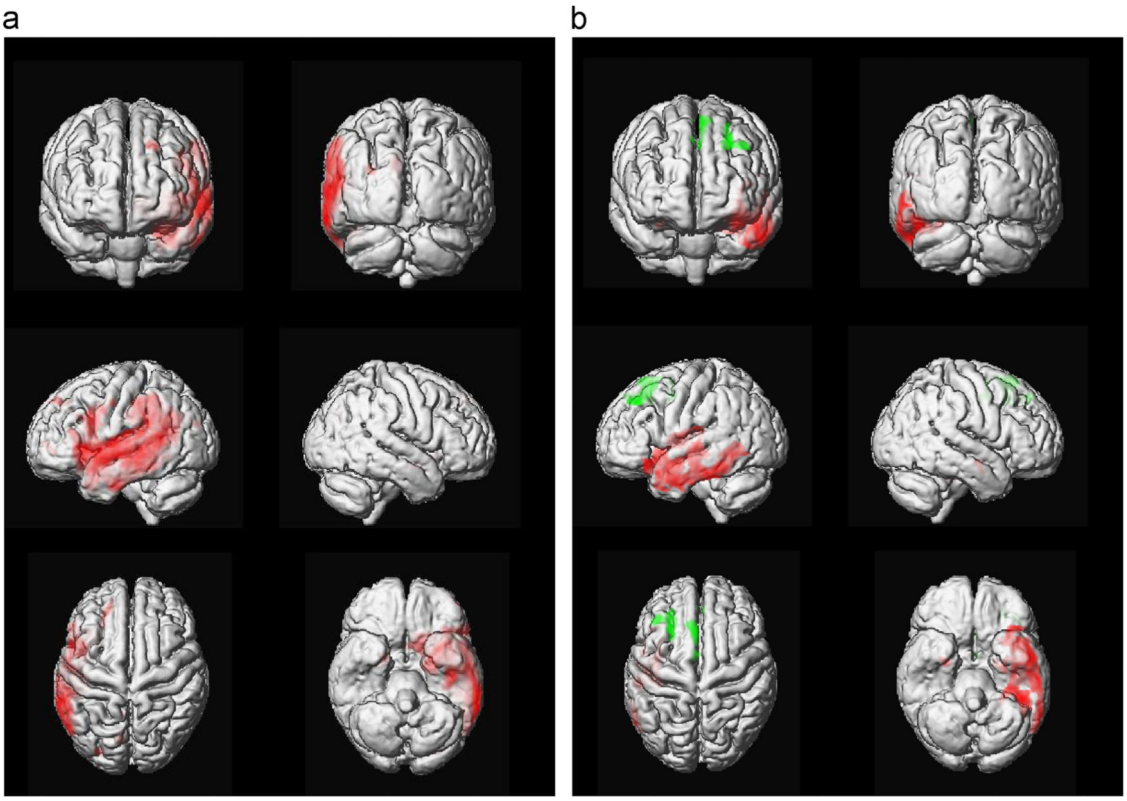


**Fig. 2.**

Gray matter atrophy in PA compared with controls. (a) Pattern of atrophy in PPA compared with controls. Areas of significant decline of gray matter volume in PPA patients compared with controls (at least 50 contiguous voxels with $p < 0.001$, uncorrected) in red projected on the rendered surface of the template brain in MNI space. (b) Gray matter atrophy specific to SD (masking out PNFA) and PNFA (masking out SD). Areas of significant decline of gray matter volume in SD patients after masking out the effect of PNFA patients in red, and decline of gray matter in PNFA patients after masking out the effect of SD patients in green compared to controls (at least 50 contiguous voxels with $p < 0.001$, uncorrected) projected on the rendered surface of the template brain in MNI space.

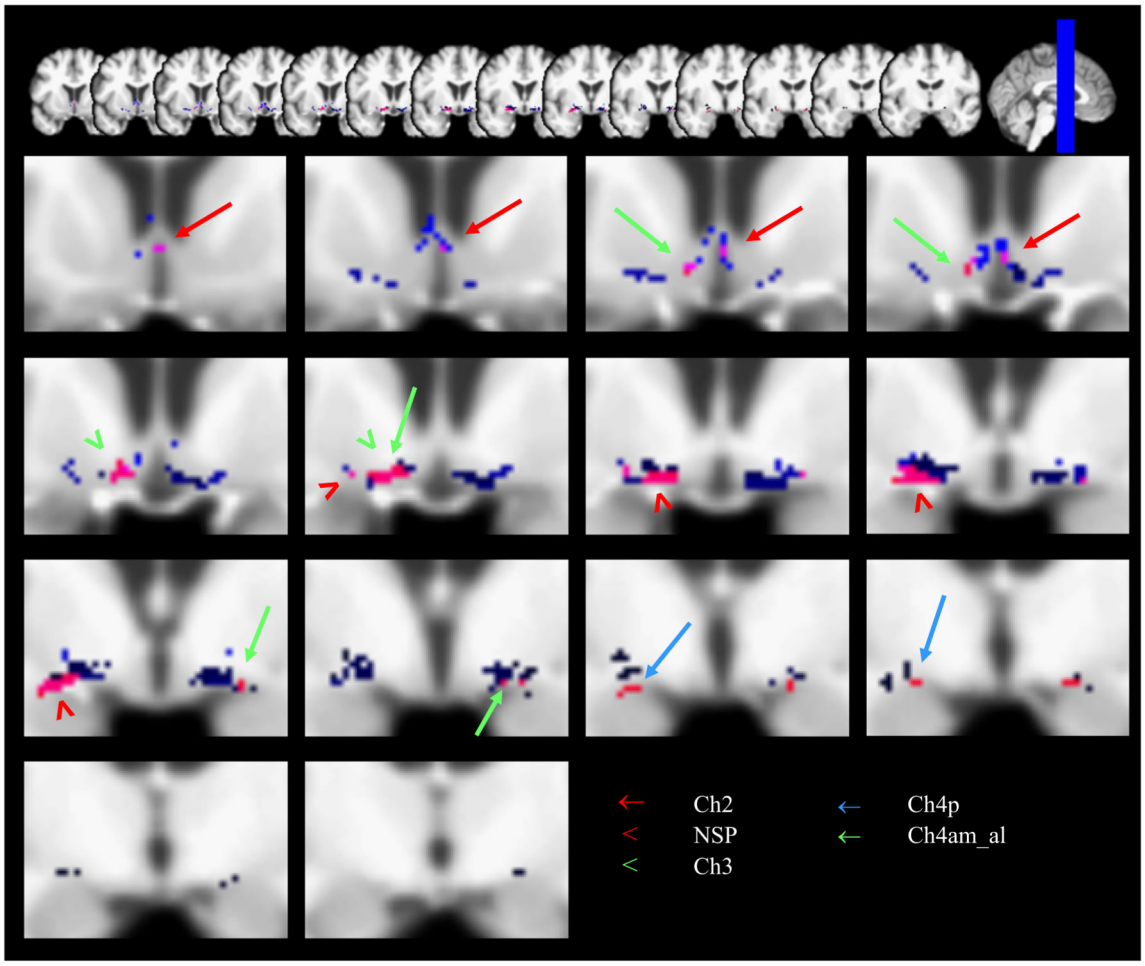


**Fig. 3.**

Effects overlaid on the post-mortem cholinergic basal forebrain map in MNI space. Coronal sections from MNI coordinates *y*=11 to *y*= −9, sections are 1.5 mm apart. Left of image is left of brain (view from posterior). The nuclei of the cholinergic basal forebrain from the post-mortem brain are overlaid on the sections in blue including the nuclei from Ch2 to Ch4p. Effect of gray matter volume reductions in PPA patients compared with controls (at least five contiguous voxels with $p < 0.01$, uncorrected) in pink. Arrows and arrow heads in different colors point to the effect in a specific subnucleus region, as outlined in the lower left corner. Effects occur almost exclusively in the left hemisphere.

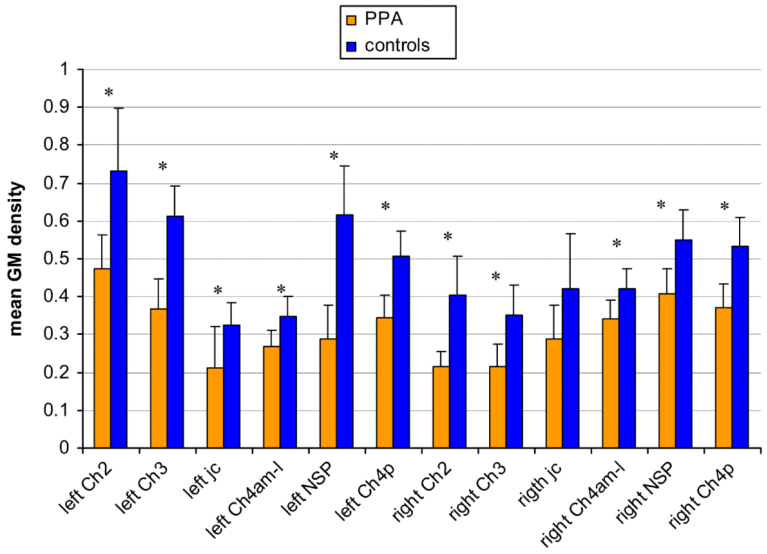


**Fig. 4.**

Regional gray matter volumes in cholinergic nuclei of PPA patients and controls. Bar graph with error bars (1 S.D.) of regional gray matter volumes of PPA patients and controls in the six subregions of the basal forebrain, corresponding to Ch2, Ch3, juxtacommissural nucleus (jc), Ch4am-al, nucleus subputaminalis (NSP), and Ch4p in both hemispheres. Significant group differences at $p < 0.001$ are indicated with an asterisk.

## Table 1

Decrease of cortical gray matter volume in PPA patients compared with controls.

| Region | Side | BA | Coordinates (mm) | | | $t_{26}$ |
|---|---|---|---|---|---|---|
| | | | *x* | *y* | *z* | |
| Middle temporal gyrus | **L** | **21** | **− 62** | **− 28** | **− 4** | **11.47** |
| Middle temporal gyrus | L | 21 | −58 | −9 | −7 | 9.48 |
| Middle temporal gyrus | L | 21 | −65 | −31 | −11 | 9.21 |
| Cuneus | **L** | **7** | **− 7** | **− 68** | **30** | **5.4** |
| Posterior cingulate | L | 30 | −7 | −60 | 14 | 3.84 |
| Middle frontal gyrus | **L** | | **− 21** | **37** | **35** | **4.53** |
| Superior frontal gyrus | L | | −16 | 46 | 38 | 4.32 |
| Cuneus | **L** | | **− 27** | **− 82** | **25** | **4.38** |
| Precuneus | **L** | | **− 6** | **− 49** | **33** | **4.29** |
| Parahippocampal gyrus | **R** | | **18** | **− 2** | **− 14** | **4.07** |
| Inferior frontal gyrus | **L** | | **− 45** | **44** | **− 3** | **3.67** |
| Inferior frontal gyrus | L | | −42 | 48 | 2 | 3.62 |

The height threshold was set at $p < 0.001$, uncorrected for multiple comparisons. The cluster extension representing the number of contiguous voxels passing the height threshold was set at > 50.

Coordinates in bold delineate a cluster and the peak *t*-value (d.f.=26) within the cluster. Subsequent non-bold coordinates identify further peaks within the same cluster that meet the significance level.

Brain regions are indicated by the Talairach and Tournoux (1988) coordinates *x*, *y* and *z*. *x*=the medial to lateral distance relative to midline (positive=right hemisphere); *y*=the anterior to posterior distance relative to the anterior commissure (positive=anterior); and *z*=superior to inferior distance relative to the anterior commissure–posterior commissure line (positive=superior).

R/L=right/left.

BA=Brodmann area.